R&D proposal for a prototype Muon Telescope Detector

Patricia Fachini, Haidong Liu, Paul Sorensen, Zhangbu Xu
Brookhaven National Laboratory, Upton, NY 11973

Hank Crawford, Jack Engelage
Space Sciences Laboratory, University of California at Berkeley, CA94720

Gerard Visser
Indiana University Cyclotron Facility, Bloomington, IN 47408

Guoji Lin, Dick Majka, Nikolai Smirnov
Yale University, New Haven, CT 06520

1)Physics Motivation

a) Intermediate mass dimuon from Drell-Yang, QGP radiation, QGP resonances, initial lepton production

One of the long-term goal of heavy ion physics as stated in STAR whitepaper is to
develop thermometers for the early stage of the collisions, when thermal equilibrium is first established. In order to pin down experimentally where a thermodynamic transition may occur, it is critical to find probes with direct sensitivity to the temperature well before chemical freezeout. Promising candidates include probes with little final-state interaction: direct photons -- measured down to low momentum, for example, via $\gamma-\gamma$ HBT, which is insensitive to the large π^0 background -- and thermal dileptons. The former would require enhanced pair production tracking and the latter the introduction of hadron-blind detectors and techniques.

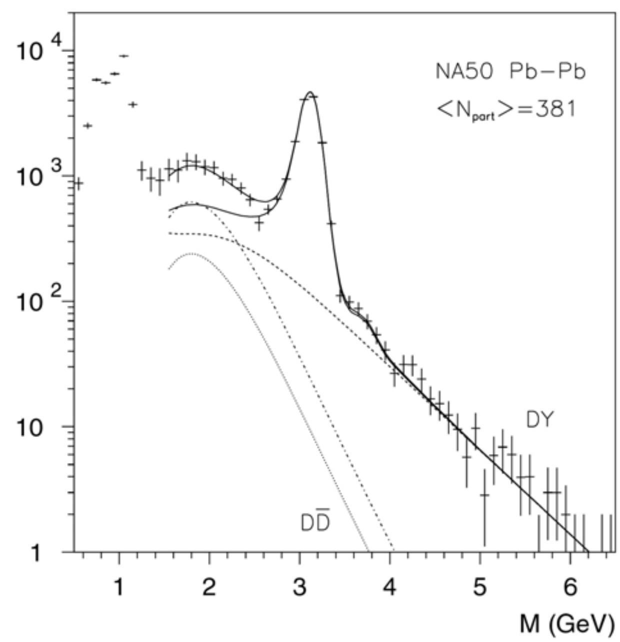

Fig.1 Dimuon invariant mass in Pb+Pb collisions at SPS

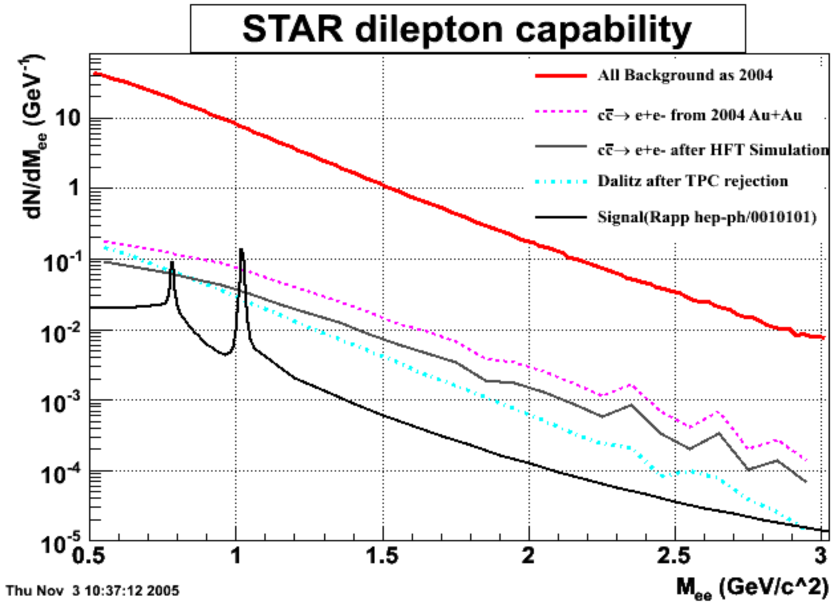

Fig.2 Dielectron Invariant Mass from simulation based on run4 data. This shows that c+cbar->e+e- dominates after background rejection from gamma conversion and Dalitz decays

b) Quarkonium

One of the short-term future measurements as requested by STAR whitepaper:

Measure charmonium yields and open charm yields and flow, to search for signatures of color screening and partonic collectivity.} Use particle yield ratios for charmed hadrons to determine whether the apparent thermal equilibrium in the early collision matter at RHIC extends even to quarks with mass significantly greater than the anticipated system temperature. From the measured p_T spectra, constrain the relative contributions of coalescence vs. fragmentation contributions to charmed-quark hadron production. Compare D-meson flow to the trends established in the u, d and s sectors, and try to extract the implications for flow contributions from coalescence vs. possibly earlier partonic interaction stages of the collision. Look for the extra suppression of charmonium, compared to open charm, yields expected to arise from the strong color screening in a QGP state (see Fig.~\ref{LQCD-screening}).

c) Hadron trigger at high pT

One of the short-term future measurements as requested by STAR whitepaper:

Establish that jet quenching is an indicator of parton, and not hadron, energy loss. Extend the measurements of hadron energy loss and di-hadron correlations to higher p_T, including particle identification in at least some cases. Do the meson-baryon suppression differences seen at lower p_T truly disappear? Does the magnitude of the suppression remain largely independent of p_T, in contrast to expectations for hadron energy loss? Does one begin to see a return of away-side jet behavior, via punch-through of correlated fragments opposite a higher-p_T trigger hadron? Improve the precision of di-hadron correlations with respect to the reaction plane, and extend jet quenching measurements to lighter colliding nuclei, to observe the non-linear dependence on distance traversed, expected for radiating partons. Measure the nuclear modification factors for charmed meson production, to look for the ``dead-cone'' effect predicted to reduce energy loss for heavy quarks.

d) Electron-muon correlation to measure the background c+cbar->l+l- correlation at intermediate mass range

It has been well-known that at RHIC, there is a source of irreducible background in dilepton invariant mass distribution at intermediate mass range. That is the lepton pair from charmed hadron semileptonic decay where the charm quark and its antiquark are pair-produced and therefore have momentum correlation. This is the dominant background at IMR. An electron-muon correlation will directly measure this background since charmed hadron pair have almost identical branching ratio to ee,μμ and 2*eμ.

2) Simulations

We has done some simulations with STAR year2003 geometry with full configuration of the current detectors and material budget. We created a pseudo-detector with 2cm thick scintillator covering the whole iron bars within |eta|<1 and leave the gaps in-between uncovered. Fig.3 is a cross-section in x-y plane of STAR detector with muons (left panel) and pions (right panel) at 1<pT<10 GeV/c. This shows graphically that muons can easily penetrate the magnet return iron bars while most of the pions will be either stopped or create shower in the irons.

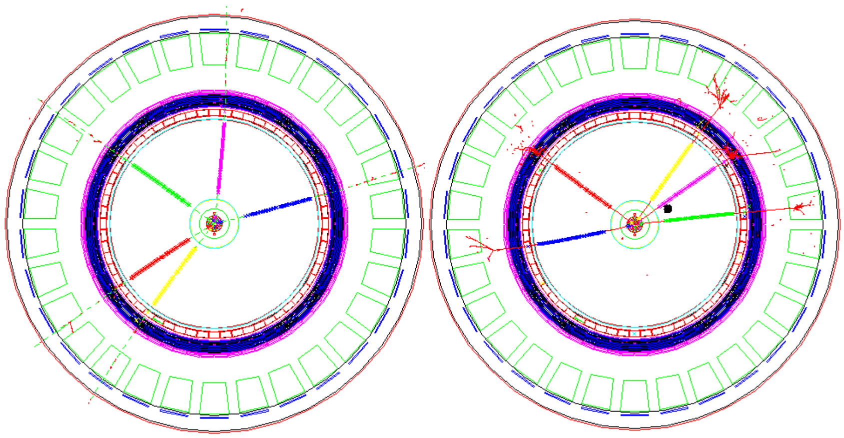

Fig.3 Examples of single muon and pion tracks in TPC

In one of the simulation setup, we generated one particle per event and collected hits information in the pseudo-MTD. Fig.4 shows fractions of the muons and pions at a given pT and random phi angle creating any hits in the pseudo-MTD. Since the pseudo-MTD covers only 73% of the phase space, it means that almost all the muons generate hits at MTD and most of the pions are absorbed by the material and only at very high pT (~10 GeV/c) significant fraction of pions is able to penetrate or create a shower reaching MTD. To achieve greater than a factor of 100 hadron rejection power from MTD at intermediate pT (1—5 GeV/c), we need to look at the hit information and use specific characteristics of the hit to further reduce the background.

In the following paragraphs, we explored cuts on time-of-flight, position relative to the track projection, and energy loss in the detector (dE/dx).

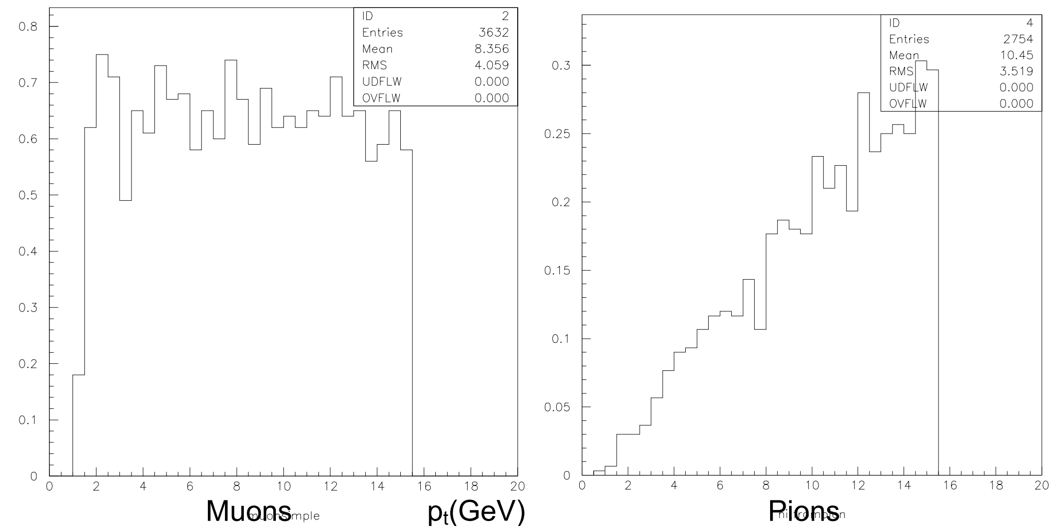

Fig.4 Fractions of muon and pion with hits in the MTD vs pT without additional cuts. MTD has 73% of the coverage avoiding the gaps of the magnet return iron bars

Fig.5 shows that all the muon hits arrive within 20ns while >90% of the pion hits arrive later and it has a long tail. We realized then that timing is a crucial selection for background rejection and this is an important feature which will determine our choice of detector. We need to further investigate the timing structure within this 20ns and see if further coincidence between expected timing from track projection and the measured time-of-flight at ~100ps scale.

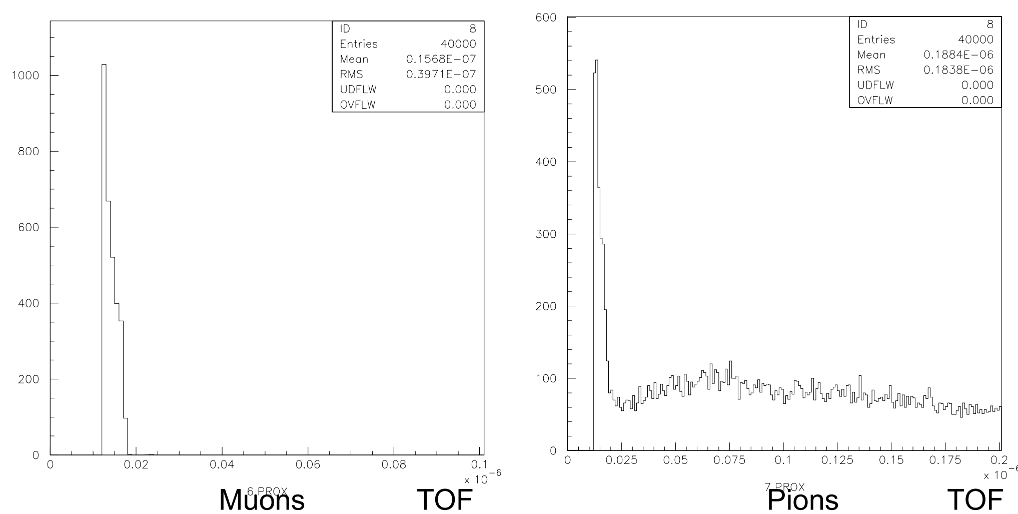

Fig.5 Timing structure of the MTD hits from muons and pions

Fig.6 shows pT vs the DCA between the hit position in pseudo-MTD and a simple helix projection of the track from TPC. At pT>4 GeV/c, the DCA from muons are within a few centimeters, while those of pions look random. Due to non-uniform magnetic field outside TPC and multiple scattering, the muon DCA at low pT is wider. Further improvement is needed for a better evaluating of the matching. For now, we use DCA<5cm for pT>4 GeV/c and DCA<10 cm for pT<4 GeV/c in any discussions involving DCA cuts.

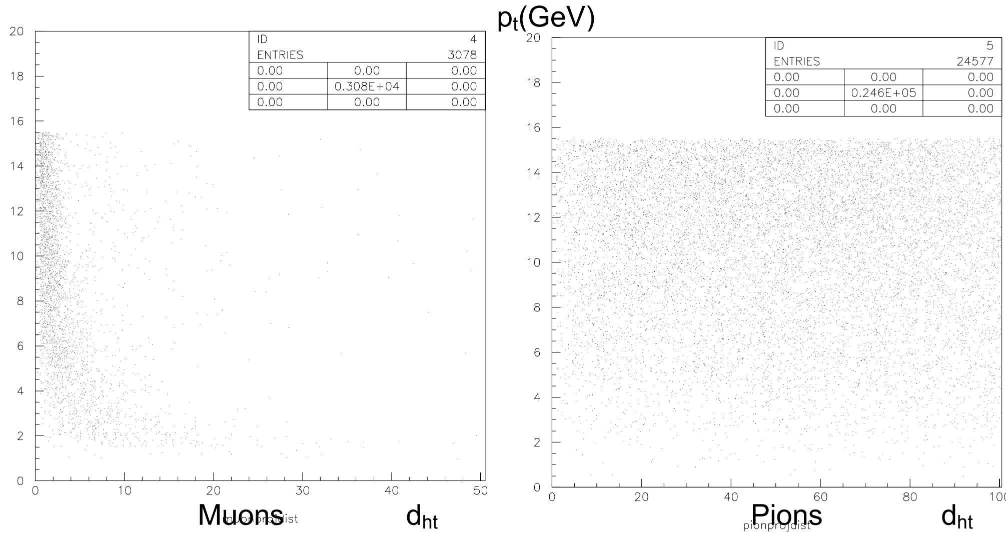

Fig.6 Distance between the hit position in MTD and a simple helix projection of the track from TPC.

Fig.7 shows the dE/dx of all the MTD hits associated with the muon or pion. The distributions suggest quite high rejection can be achieved with dE/dx cut.

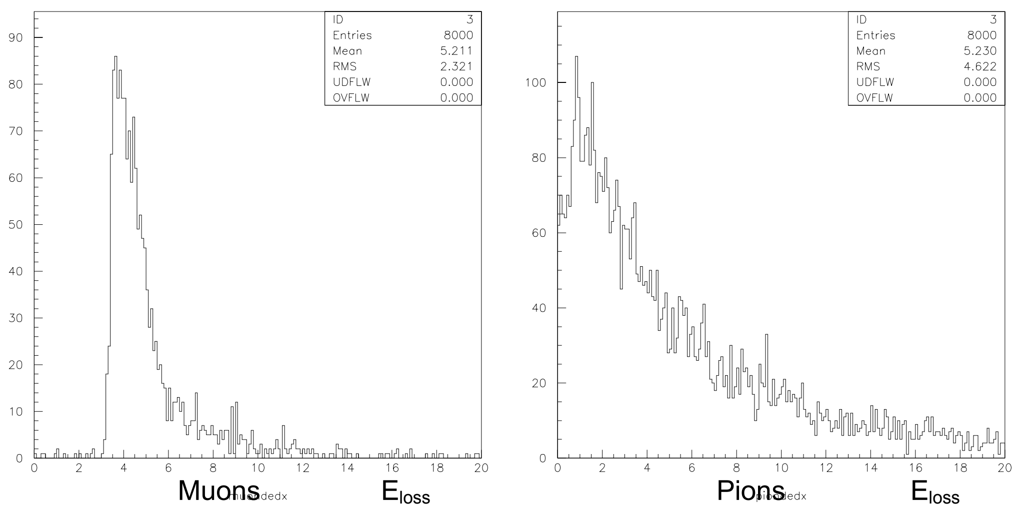

Fig.7 The muon dE/dx in MTD and the dE/dx of all particles associated with a primary pion.

To fully access the potential of MTD on the muon identification and trigger capability, we ran HIJING events through the GEANT for STAR (starsim). Fig.8 is a full HIJING central Au+Au collisions. This shows that most of the particles are stopped before the barrel EMC and most of the escaping particles (primary or secondary) are through the gaps of the iron bars.

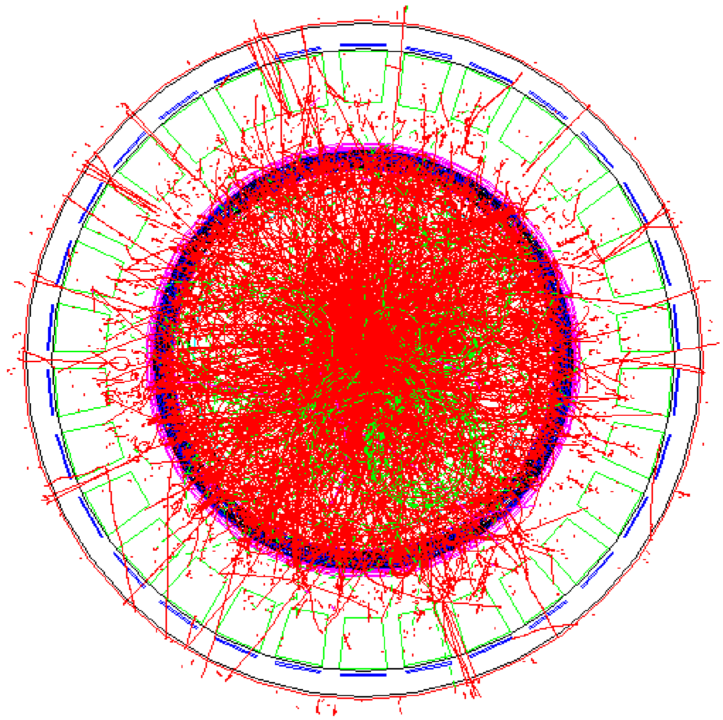

Fig.8 Full HIJING central Au+Au collisions simulated with year2003 geometry.

Fig.9 shows pT distribution of the particles in central HIJING Au+Au collisions (left panel) and those tracks projected with a MTD hit which may not necessarily created by the particle itself due to random coincidence between a track projection and a MTD hit(right panel). The low pT part is due to track projection randomly matching with a hit created by an energetic particle. Since there are many soft particles, the random coincidence is high. However, we are not interested in low momentum tracks and a track selection with pT>1.5 GeV/c will reduce these coincidences. We see 840 hadrons created in 100 central Au+Au HIJING events with pT>2 GeV/c and only 3 survive the selections in MTD. This means that using the simple algorithm, we can achieve hadron pion rejection power at about 200. In addition, the TOF will be able to reject all the kaons and protons, and TPC dE/dx at 8% resolution will enhance the muon/pion selection by a factor of 2. These together give us a 10^3 muon-to-hadron enhancement.

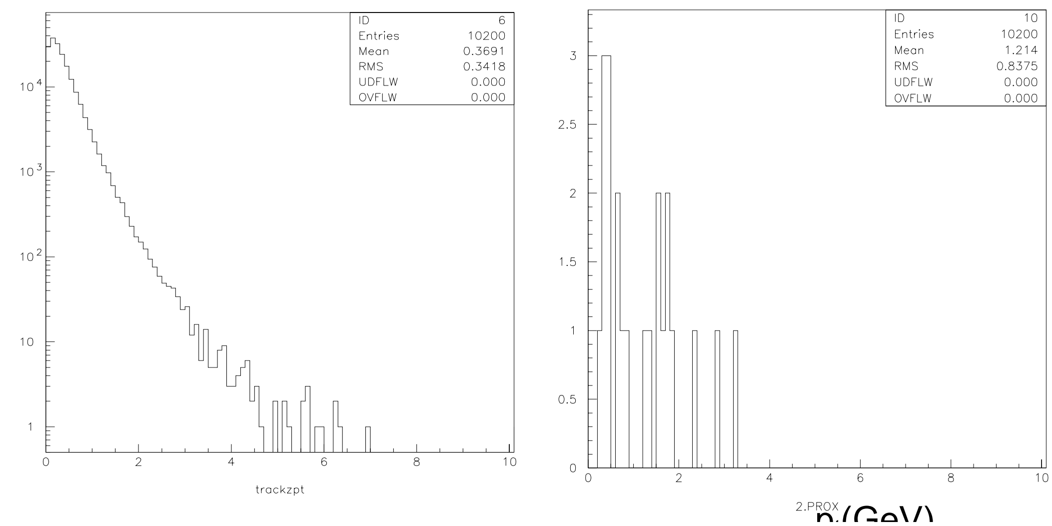

Fig.9 HIJING input particle pT distribution and the pT distribution of particles matching with MTD hits, which includes random coincidence.

We also examine the possibility of online trigger on the muon detector. Table.1 list the hits per event after TOF and/or dE/dx cuts described above. Now we can achieve a factor of 6 enhancements on a dimuon trigger. Further studies with finer timing cut (at ~100ps level) should be explored to see if it is possible to perform this at L0 or L2.

Cuts	**Nhit/event**
No cut	**70**
TOF	**1.6**
Eloss	**7.6**
TOF&Eloss	**0.72**

Table 1: Hits per central HIJING event for different cuts.

3) Additional Simulation required

a) continue to improve the simulation with muon identification: tighter timing cut, space resolution cut.

We need to further investigate the timing structure within the 20ns and see if further coincidence between expected timing from track projection and the measured time-of-flight at ~100ps scale.

b) Improve the track projection. Now a helix is used from TPC all the way to the MTD, however the field between TPC and MTD is far from uniform. This will mainly improve the track-hit matching at low momentum.

c) Explore the possibility of filling the gaps between the iron bars with aluminums to increase the effective coverage

d) Need to develop an algorithm to select high-pt hadrons which either penetrate or develop a shower reaching MTD.

4) Test Muon Telescope Detector for run 6

We have installed a test MTD using two spare CTB trays. The trays are attached to the HV box outside the iron bars and are separated by 35cm radically. Fig.10 and Fig.11 are picture and engineer drawing of the test MTD in STAR. In run6 p+p collisions, we plan to make a three-way coincidence between the two MTD trays and the 6 of the half inner CTB trays aligned to the beam line. The goals of the run6 test MTD are:

1) study the background rate
2) study the background timing pattern
3) study DCA of background muon from pi/kaon decay
4) possible non-background muon spectrum

Fig.10 a test MTD using two spare CTB trays. The trays are attached to the HV box outside the iron bars and are separated by 35cm radically.

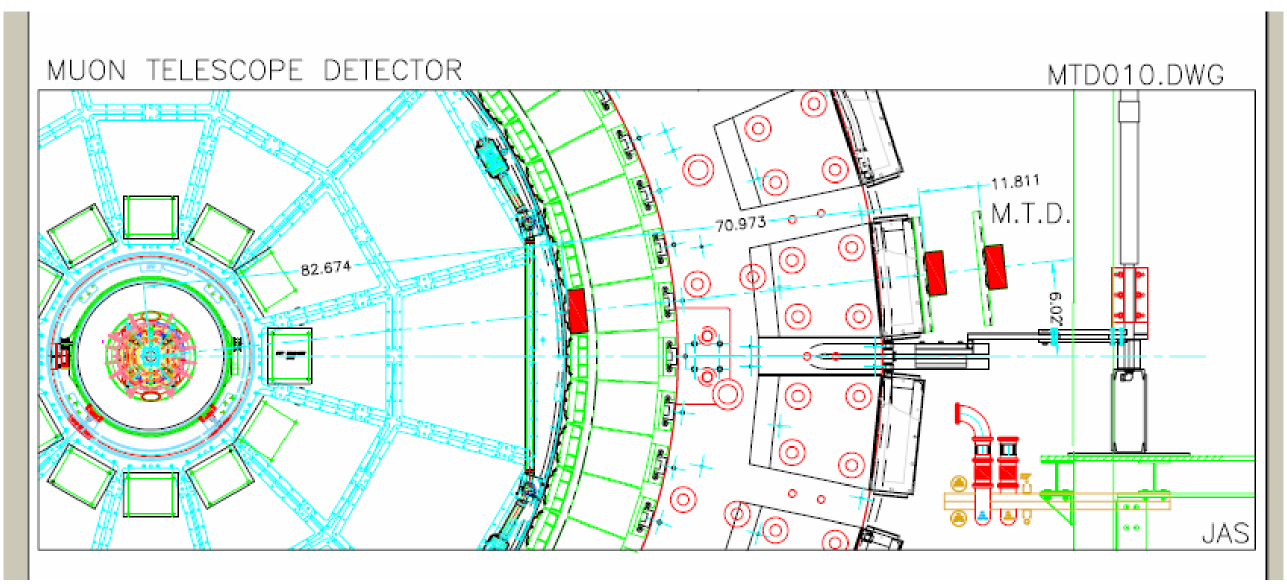

Fig.11 Engineer drawing of the test MTD

5) R&D of a new MRPC muon detector

Detector requirements:
i) Large Coverage (cost-effective)
ii)Time (< ns)
iii) Spatial resolution (<cm)
iv) Some dE/dx capability
v) Tracking capability?

Possible candidates:

a)Scintillators
b)RPC
c)MRPC (long strips, two-end readout)
d) Proportional Wire Chamber
e) Straw Station?
f) Some Combinations of above or others?

Trigger and Electronics:
Further studies with finer timing (at ~100ps level) should be explored to see if it is possible to perform this at L0 or L2.

Although most of the hardware is reasonably easy to build, we are inclined to use MRPC for the full coverage (cost-effective) and this has never been used as a muon detector.

6)A three-layer prototype MTD

we propose to build a prototype MTD with three layers:
a) R&D on MRPC with Large module, long strip and two-end readout
ALICE uses 8cmx1.2m MRPC with 3x6 pads
There is proposal for FAIR/GSI with long strip readout.
Part of the NSLS electron test beam we setup for the TOF test
(gas system, readout etc.) can be used for this test.

b) wire chambers (Nikolai has two and Dick has the readout from E864)
We have two MWPC in a "working condition".
Size (active area): 12x12"
Read-out: anode wires; connected in 12 strips / Chamber.
Cathode strips; 0.2" width, 56 / Chamber.
Gas: Ar+CO2(30%), the simplest gas system.
HV: "+" polarity, ~2 kV.
FEE: readout for E864 straw chamber stations

c) Scintillator (we have two spare CTBs and will have more next run)

d) R&D on L0 trigger from MRPC readout.

A Fast Time-to-Digital Converter for STAR

A high-speed time-to-digital converter would have many potential applications in STAR, including the muon telescope detector, a vertex position detector, a start detector for TOF; basically, anywhere that a timing measurement or timing cut is desired as input to the L0 trigger or any other fast hardware. Besides the time resolution, the key specifications of interest include the digitization time, measurement range (preferably 100% live, or else some fixed portion of RHIC strobe period), recovery time / double-pulse resolution, linearity, and tolerance to RHIC strobe jitter.

Based on a design prototyped by G. Visser some years ago at LBL for a proposed vertex position detector, we would address the above requirements with a pipelined time-to-digital converter consisting of a TAC, ADC, and FPGA-based digital signal processing. The coarse timing (to ticks of an 80 MHz clock) is provided by the FPGA, and time interpolation is provided by the TAC, which generates a trapezoidal pulse output with a precision baseline and leading edge slope. If a the leading edge is digitized by a 10-bit ADC with 9.3 ENOB, and the leading edge slope is 80% of the ADC full scale range per clock period, then the event time can be interpolated to 25 ps. Specifically, the dual-channel AD9216 would be a good choice for this application. Jitter in the clock source and ADC have to be held to <5 ps to achieve this, but this is well within standard technology. A 12-bit ADC could interpolate comfortably to about 10 ps, if that is required. The TAC itself would consist of a constant current source, an active integrator with differential output, and a Schottky diode bridge reset switch. Such a switch, used on the EEMC MAPMT front-end electronics and soon on the FMS front end electronics, opens very quickly and cleanly with little charge injection. The input edge to be timed opens the reset switch, and it is reclosed when the integrator saturates. Reclosure timing is not critical – it does not affect the current measurement – but the TAC must settle quickly enough to meet the recovery time or double-pulse resolution specification. Experience from the EEMC design indicates that it can settle to full accuracy in <35 ns. This means that two edges separated by at least (12.5 ns)/0.8+(30 ns) = 51 ns *can be independently measured to full accuracy*. Of course, if this is not required, it can possibly be traded off for some cost or power savings. The FPGA's job is to read the digital data stream from the ADC, discriminate when an event occurred, count the coarse time, interpolate the fine time from the point(s) measured on the linear leading edge (applying calibrations), and process the data for L0 trigger input (as a minimum, it would have to assign the edge to a particular RHIC strobe cycle and retime the digital data for input to the DSM tree). Final digitized time data, to any reasonable number of bits, e.g., 24 bits @ 25 ps = 420 μs, is available after about 11 clock cycles (1 used for TAC, 6 for the ADC, in case of AD9216, and 4 for the FPGA) – that is 138 ns.

The actual time of the RHIC strobe would be measured on each cycle (taking advantage of the excellent double-pulse resolution of this architecture); it is treated as just another potentially random quantity to be measured. Calibration data would be taken on each channel using a built-in test pulser, based on a clock of slightly different frequency, e.g., 80.000001 MHz, and a prescaler. It is only a baseline and gain correction that needs to be applied – unlike some competing TDC technologies, e.g., chain-of-gates type time interpolator, the time calibration is set by a ratio of just two circuit elements (the current source and the integration capacitor) independent of which event or the exact time of the event. So there will be no wiggles or nonlinearities that need to be compensated.

One channel of the above described (10-bit) electronics would occupy about 7 mm x 100 mm of area on a 4- or 6-layer printed circuit board, and would have a power dissipation approximately 200 mW and a component cost approximately $21, exclusive of connectors, mechanical/enclosure, and power supply, and of course exclusive of engineering & development costs.

The detector will have these three layers on top of each other to evaluate
the performance of each other in run7 and/or run8.

7) R&D Budget

a) MPRC with large area, long trips

b) Electronics for L0 and L2 trigger with good timing

c) Prototype installation and integration

d) manpower and computers for crucial additional simulations
These (item d) can be provided by other budgets but is crucial for the success of the project.

8) Summary

A large-area muon detector at mid-rapidity in STAR will be crucial for the advance of our knowledge of QGP. It directly addresses the open questions and long-term goals proposed in STAR white paper on "Experimental and Theoretical Challenges in the Search for the Quark Gluon Plasma: The STAR Collaboration's Critical Assessment of the Evidence from RHIC Collisions". Specifically, it allows us to measure intermediate mass dimuon from Drell-Yang, QGP radiation, QGP resonances, initial lepton production, quarkonia and possible high-pT hadron.

However, many questions and features of the detectors and background have to be explored. We therefore propose a R&D project for a muon telescope detector (MTD) to address these issues and try to find a cost-effective configuration. We propose to build a prototype MTD with three layers: MRPC TOF + Wire Chamber + CTB trays outside the STAR magnet. Detector and electronics R&D and further simulations are necessary for a large-area muon detector.